

Design and implementation of site-specific rainfall-induced landslide early warning and monitoring system: a case study at Nam Dan landslide (Vietnam)

Quoc Anh Gian, Duc-Tan Tran, Dinh Chinh Nguyen, Viet Ha Nhu & Dieu Tien Bui

To cite this article: Quoc Anh Gian, Duc-Tan Tran, Dinh Chinh Nguyen, Viet Ha Nhu & Dieu Tien Bui (2017) Design and implementation of site-specific rainfall-induced landslide early warning and monitoring system: a case study at Nam Dan landslide (Vietnam), Geomatics, Natural Hazards and Risk, 8:2, 1978-1996, DOI: [10.1080/19475705.2017.1401561](https://doi.org/10.1080/19475705.2017.1401561)

To link to this article: <https://doi.org/10.1080/19475705.2017.1401561>



© 2017 The Author(s). Published by Informa UK Limited, trading as Taylor & Francis Group.



Published online: 21 Nov 2017.



[Submit your article to this journal](#)



Article views: 247



[View related articles](#)



[View Crossmark data](#)



Design and implementation of site-specific rainfall-induced landslide early warning and monitoring system: a case study at Nam Dan landslide (Vietnam)

Quoc Anh Gian ^{a,b}, Duc-Tan Tran ^a, Dinh Chinh Nguyen^a, Viet Ha Nhu^c and Dieu Tien Bui ^d

^aFaculty of Electronics and Telecommunication, VNU University of Engineering and Technology, Hanoi, Vietnam; ^bDepartment of Electronics, Nam Dinh University of Technology Education, Nam Dinh, Vietnam; ^cDepartment of Geological-Geotechnical Engineering, Hanoi University of Mining and Geology, Hanoi, Vietnam; ^dGeographic Information System group, Department of Business and IT, University College of Southeast Norway, N-3800, Bø i Telemark, Norway

ABSTRACT

This paper proposes and implements an early warning and monitoring system for rainfall-induced landslide (named as EWM_{RIL}) with a case study at the Nam Dan landslide (northern Vietnam). The proposed system consists of six sensor nodes and one rainfall station that are used to sense large amounts of data in real-time such as soil moisture, pore-water pressure (PWP), movement status, and rainfall. In addition, a new flexible configuration for the wireless communication system is proposed that is capable not only to save the energy consuming but also to ensure the reliability of the system. Using wireless communication system, the sensed data were sent to the computer station for analyzing and predicting the instability of the landslide in terms of factor of safety (FoS) using the finite element seepage analysis and the limit equilibrium slope stability analysis methods. These methods are available in the SEEP/W and SLOPE/W modules of the GeoStudio software. Based on the analyzing results, the system proposed three warning levels for the landslide Early, Intermediate, and Imminent. Experiment result in the rainy season from August to September 2016 has proven the validity of the EWM_{RIL} system. The result of this study is useful for landslide risk prevention and management in landslide prone-areas.

ARTICLE HISTORY

Received 12 July 2017
Accepted 31 October 2017

KEYWORDS

Early warning; landslides;
finite element method;
GeoStudio; Vietnam

1. Introduction

Rainfall-induced landslide is one of the most serious natural hazard problems in mountainous areas because it may suddenly occur with high travelling speeds posing threats to human life and properties (Kirschbaum et al. 2009), and especially, to building and infrastructures (Ahlheim et al. 2008; Klose et al. 2015; Del Soldato et al. 2017; Loi et al. 2017). Annual direct and indirect economic losses and casualties were estimated over \$1 billion in many countries i.e. Japan, China, Italy, and the United States (Schuster and Fleming 1986; Xie et al. 2005; Kjekstad and Highland 2009; Trezzini et al. 2013).

Due to changes of climate i.e. high frequency of rainstorms (Barla and Antolini 2016; Tien Bui et al. 2016), fast population growth with uncontrolled urban sprawl, and improper settlement development, frequency and trend of landslide occurrence are increased and reached an alarming rate in

many countries (Saito et al. 2014; Dou et al. 2015; Ávila et al. 2016; Lin et al. 2016; Wood et al. 2016). This problem is of particular concern in Vietnam, where landslides occurred in almost all mountainous areas due to high frequency of tropical rainstorms in recent years (Pham et al. 2017; Loi et al. 2017; Tien Bui and Anh Tuan et al. 2017; Tien Bui and Nguyen et al. 2017). Therefore, studying of landslides to determine measures for landslide risk prevention and management is highly necessary. These have been clearly stated in the guidelines for risk analysis and sustainable disaster management within International Strategy for Disaster Reduction of United Nations (UN-ISDR 2006).

Among various methods for the landslide risk prevention, monitoring and early warning systems are considered to be one of the most promising ways (Uchimura et al. 2015). Literature review shows that various monitoring and early warning systems for rainfall-induced landslides have been successfully proposed, from national to site-specific scale with different time spans i.e. short term, medium term, or long term. For national and regional scales, early warning systems are built mainly based on the established relationships between rainfall intensity/duration and the consequent activation of landslides (Baum and Godt 2010; Liao et al. 2010; Lagomarsino et al. 2013; Papa et al. 2013; Mathew et al. 2014; Manconi and Giordan 2015; Calvello and Piciullo 2016). However, monitoring of only rainfall for evaluating the failure for individual slopes is not enough because the shear strength of these slope materials is not always the same.

For site-specific scale, early warning systems are mostly based on near-real-time monitoring of slope movement and triggering variables at the site, i.e. rainfall and pore-water pressures (PWP) (Yin et al. 2010; Thiebes et al. 2014). Accordingly, thresholds for alarming could be determined either by experts through the interpretation of monitoring data (Intrieri et al. 2012) or the use of physical or numerical models (Capparelli and Versace 2011). The later one that integrates directly monitoring data and numerical models has been considered effective systems for landslide early warning, and for this case, networks of sensors for monitoring landslide triggering factors must be constructed. Some successful integration models can be seen as infiltration models (Greco et al. 2010; Capparelli and Versace 2011; Chae and Kim 2012), slope equilibrium models (Thiebes et al. 2014), and slide propagation model (Yin et al. 2010; Macciotta et al. 2016). Nevertheless, detailed development of rainfall-induced landslide warning systems for site-specific scale is still rare. More importantly, flexible, innovative designs and detailed technical explanations for the establishment of wireless networks of sensors for monitoring and early warning systems for rainfall-induced landslides have been seldom provided.

This work aims to partially fill this gap in the literature by proposing an early warning and monitoring system for rainfall-induced landslide, named as EWM_{RIL}, with a case study at landslides in the north of Vietnam. In this paper, the detailed design and implementation of the wireless sensor network (WSN) for monitoring landslide triggering parameters were provided. These monitoring data were integrated with a predictive model that was constructed using the finite element method (FEM) (Quecedo et al. 2004).

2. Background of the methods, sensors, and wireless networks used

To implement a rainfall-induced landslide warning system, it is necessary to determine the instability status for the landslide being considered, and for site-specific landslides, the instability status can be determined using factor of safety (FoS) (Collins and Znidarcic 2004). Thus, FoS could be monitored and assessed using wireless sensors network and GeoStudio software installed in a monitored station. This section describes the theoretical background of FoS, the software used for calculating FoS, and the proposed wireless sensors network used.

2.1 Factor of safety

According to Rahimi et al. (2010), the calculation of FoS for a landslide can be carried out by two steps: (i) in the first step, finite element seepage (FES) analysis is conducted to estimate PWPs of the

landslide, based on soil–water characteristic curve and permeability function; (ii) in the second step, the limit equilibrium slope stability (LESS) analysis is performed to compute unsaturated shear strength parameters, and then, estimating FoS for that slope.

It is noted that the FES and LESS analyses in this study are carried out using the commercial software packages of SEEP/W (Krahn 2012a) and SLOPE/W (Krahn 2012b) in the GeoStudio, respectively. Accordingly, the PWP is calculated using the water-flow governing equation (Rahimi et al. 2010) as follows:

$$\frac{\partial}{\partial x} \left(k_x \frac{\partial h}{\partial x} \right) + \frac{\partial}{\partial y} \left(k_y \frac{\partial h}{\partial y} \right) + q = m_w^2 \gamma_w \frac{\partial H}{\partial t} \quad (1)$$

where h is the hydraulic head available for flow, k_x is the coefficient of permeability in x -direction; k_y is the coefficient of permeability in y -direction; H is the hydraulic head or total head; q is the applied flux at the boundary; m_w is the slope of soil–water characteristic curve, the coefficient of volumetric water change with respect to a change in negative PWP; γ_w is the unit weight of water, and t is the time.

The LESS model uses the shear strength of unsaturated soil for estimating the FoS using the following equation (Fredlund et al. 1978)

$$T_i = c' + (\delta - u_a) \tan \phi' + (u_a - u_w) \tan \phi^b, \quad (2)$$

where T_i is the shear strength at the i th slice of the slip surface; c' is the effective cohesion; δ is the total normal stress; u_w is the PWP; u_a is the pore-air pressure; $(u_a - u_w)$ is matric suction; $(\delta - u_a)$ is the net normal stress; ϕ' is the effective friction angle; and ϕ^b is the angle with respect to changes in matric suction when the net normal stress is held constant.

Once the LESS model for the landslide is determined, the FoS for the landslide is calculated as the ratio of shear strength to shear stress as follows (Liu et al. 2015):

$$\text{FoS} = \frac{T_i}{\tau_i} \quad i = 1 : N, \quad (3)$$

where N is the number of slide of the slip surface; τ_i is the effective normal stress at the i th slice of the slip surface.

2.2 Sensor and wireless networks for rainfall-induced landslide early warning system

The successful design and implementation of a rainfall-induced landslide early warning system are strongly dependent on sensors and networks used. The reason is that the sensors and networks are used to collect, handle, and transmit massive amounts of monitoring data (Ramesh 2014). Therefore, it is necessary to properly determine type of the sensors used, number and location of the monitoring points, and sampling rates of the monitored parameters (Angeli et al. 2000).

It is well-known that the selection of the sensors is dependent on triggering parameters of the landslide being considered. For rainfall-induced landslides, failures are mainly influenced by groundwater condition, rainfall intensities, and soil properties of the slope (Rahardjo et al. 2010). Accordingly, infiltration of water into the slope material during rainfall events causes increasing PWP and decreasing shear strength, and thus, reducing the FoS (Terlien 1998). Therefore, PWP sensor and soil moisture sensor should be used to collect and monitor the material characteristics of the slope for determining the instability status of the landslide.

This section describes types of the sensors used for the proposed EWM_{RIL} model. In this research, the term of ‘sensor node’ used is defined in Nguyen and Tran et al. (2015), whereas ‘network’ refers

to the logical connection between the sensor nodes. The sensors are buried underneath the slope and selected based on accuracy, response time, power consumption, and long-term usage. The sensor nodes are connected using wireless communication and data transmission protocols (López et al. 2014). Accordingly, the monitored parameters are: (i) indirect factors such as rainfall, groundwater level, moisture, and PWP in the soil within the sliding block at different depths; (ii) direct parameters such as amplitude, speed, and sliding translation direction of the slope.

Accelerometer: The aim of this sensor is to determine the tilt and the vibration of the landslide being considered. Thus, the change rate of the velocity and magnitude of the landslide in 3-axis directions through time can be monitored. The displacement rate is used to design the warning thresholds. Conventionally, geophones have been used for the analysis of vibrations of landslides such as in Ramesh (2014). However, recent studies point out that micro-electro-mechanical-systems (MEMS)-based accelerometers outperform geophones in terms of power consumption (Hons et al. 2008; Deng et al. 2014), therefore, the three-directional MEMS-based accelerometer ADXL-335 was proposed to use in this study (Bhattacharya et al. 2012). Accordingly, acceleration can be calculated using the equation as follows:

$$ACC_i = (Sam_i / 1024 \times R - O_i) / Sen_i, \quad (4)$$

where ACC_i is the acceleration value in direction i ($i = X, Y, Z$); Sam_i is the value after sampling of axis i ; R is the voltage reference; O_i is the offset, and Sen_i is the sensitivity of the accelerometer on axis i .

Bandwidths of this accelerometer can be configured within a range of 0.5–1600 Hz for X and Y axes, and a range of 0.5–550 Hz for the Z axis (Bhattacharya et al. 2012).

Rain gauge: Rainfall-induced landslide is influenced by rainfall intensity, duration, and antecedent rainfall (Tien Bui et al. 2013). In addition, in many mountainous areas, rainfall is dependent on many local factors such as topography and elevation (Chae and Kim 2012). Therefore, if available rainfall stations are far from the landslide being considered, a new rain gauge near the landslide should be established at a safe distance to the landslide for measuring rainfall data. The rain gauge connects and transmits data directly to the network's sink node.

The PWP sensor: This sensor is used to measure the pressure of groundwater of the slope. Depending on the underground structure of the slope, a number of PWP sensors should be placed at different depths to monitor the effect of both negative and positive PWP, respectively (Collins and Znidarcic 2004). Accordingly, tensiometers could be buried beneath the ground surface for measuring the negative PWPs, whereas piezometers could be installed below the groundwater level for measuring positive PWPs. In this study, we used the vibrating-wire piezometers manufactured by Slope Indicator, Inc. for measuring the PWPs.

Soil moisture sensor: One of the most important factors affecting the infiltration of soil is the amount of water (Chae and Kim 2012). In unsaturated soils, the volume of water stored within the void spaces is varied, depending on the matric suction within the pore-water. The matric suction is defined as the difference between the air (u_a) and water pressure (u_w). Therefore, the soil moisture sensor should be used to gather the volume of water in the soil. Accordingly, the volume of water content is derived indirectly through measuring the electrical conductivity of the soil medium surrounding them using the following equation

$$SM = \frac{(SM_{ADC} - OS_{ADC}) * 200}{1023 - OS_{ADC}}, \quad (5)$$

where SM is the soil moisture value (%); SM_{ADC} is the analog to digital converter (ADC) output; and OS_{ADC} is the offset value at 0 Kpa.

Wireless communication: In this study, we proposed to use XBee-Pro ZigBee module (also called XBee for short) that is based on the wireless communication standard IEEE 802.15.4 and is engineered for operating with the ZigBee protocol. The main advantage of ZigBee is that it consumes low power, therefore, it is suitable for the sensor nodes powered by battery. The XBee module has a data rate up to 250 kbps with the 2.4 GHz ISM band. Furthermore, the XBee module includes low power sleep mode (Manual Product 2008).

Microprocessor: This is a central element of a sensor node. The microprocessor controls sampling time, collects data from sensors, conveys aggregate data to the Radio Frequency (RF) module to transmit to the sink node. In these sensor nodes, where power consumption is constrained by battery capacity, the microprocessors should be a low power consumption.

WSN: This is proposed for the Rainfall-Induced Landslide Early Warning and Monitoring System because it has proven suitable for applications in environmental monitoring due to its flexibility, real-time data capture, and transmission (Baronti et al. 2007; Rawat et al. 2014; Fosslau et al. 2016). In this study, the WSN consists of six sensor nodes and one sink node. Environment parameters are measured at these sensor nodes, and then, are transferred to the sink node via wireless links. The sink node delivers the measured data to users through internet by a gateway.

3. The proposed EWM_{RIL}

3.1. Structure of the proposed early warning and monitoring system

The structure of the proposed EWM_{RIL} in this study is shown in Figure 1. First, the microprocessor units in these sensor nodes acquire the data from all sensors and transfer to the wireless interface module (Figure 2(a)), and then, the wireless interface modules send the data to the sink node and the gateway unit. In the next step, the data are uploaded to the Web Server through the gateway. Then, the data from Web Server are formatted and forwarded to the monitoring Website, the mobile phones of people in charge, and the Computer Station. Finally, the GeoStudio program at the Computer Station is used to analyze the instability status (using FoS) of the slope being considered, and its results can be used to reconfigure the WSN (see Figure 5) and give an alarm if need be.

3.1.1. The sensor node

The proposed wireless sensor node in this study includes three PWP sensors, three accelerometers, and one soil moisture sensor (Figure 2(a)). In addition, communication bus, microprocessor, pin

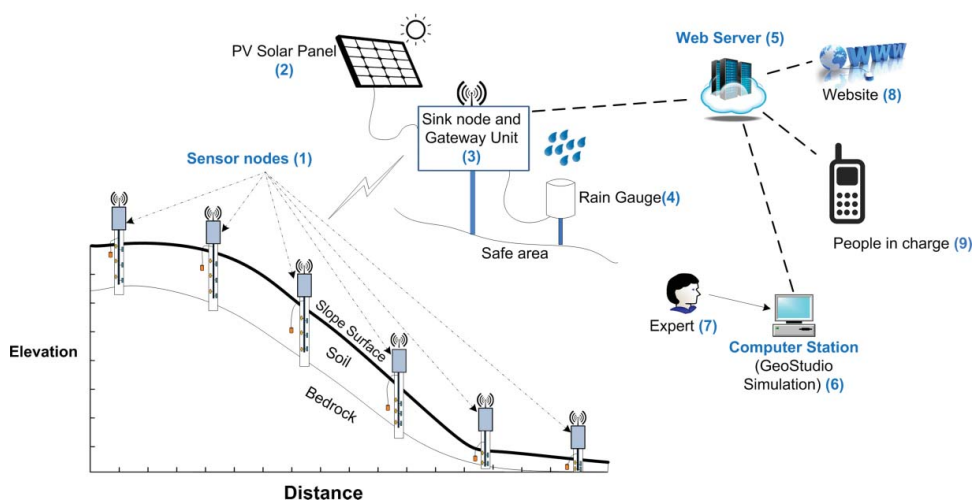


Figure 1. Diagram of the proposed system.

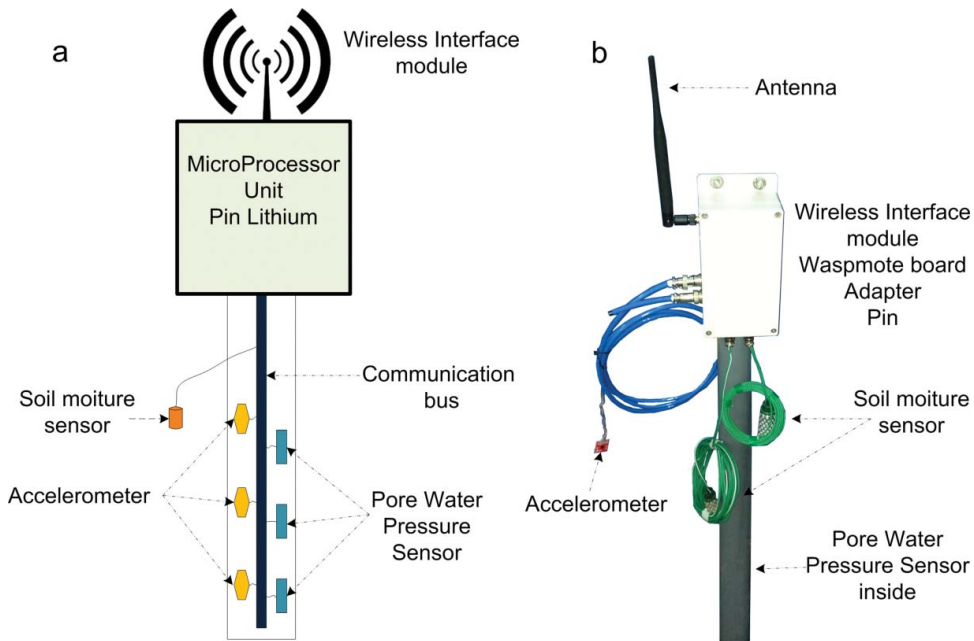


Figure 2. (a) Component of the wireless sensor node used in this study; (b) Photo of the wireless sensor node used in this study (the photo was taken by Tran Duc Tan on 10 September 2016).

Lithium, and wireless interface module are included. The detailed structure of the proposed sensor node and a photo of a real wireless sensor node are shown in Figure 2(a,b), respectively. It is noted that the topology of the network is designed to include both the star topology (Figure 3(a)) as suggested in Gutierrez et al. (2001) and the tree topology (Figure 3(b)) as proposed in Cuomo et al. (2008). The sensor node packages the monitoring data, and then the data are transferred to the sink node and the gateway unit through wireless communication (see Figure 1).

The use of both the star topology and the tree topology (Figure 3(a,b)) is important for the EWM_{RIL} system because it enables a tradeoff between the power saving and the reliability of the network. Thus, it is an effective mechanism to exploit the advantages of both topologies. The reason is that the tree topology could extend the lifetime of each sensor node, however, the system using only this topology will be broken if a cluster node is out of work due to the landslide or other errors. Data of all nodes connecting to this cluster node will not be transferred to the destination, and thus, this affects the reliability of the EWM_{RIL} system. For the star topology, every node sends the data to the sink and gateway node directly, and consequently, failures of one node do not break the system. However, the star topology consumes more power compared to that of the tree topology (Cuomo et al. 2008).

The synchronization in WSN network, which establishes a time reference among sensor nodes, is a critical point. The synchronization solution is a balance of energy efficiency, accuracy, and other factors which are weighed based on specific applications. In our system, the most important moment in the operation of the system is when the FoS is low. At this time, the network is configured as the star topology. On the other hand, the number of sensor nodes is small. The scheme used for synchronization in this research is reference broadcast synchronization (Elson et al. 2002).

In our work, we used the commercial platform for wireless sensor networks from Libelium, Spain. Waspnote has a real-time clock module which is used for setting time and alarm clock. Alarm clock part enables to set alarm clocks and get interruption to wake up. Thus, the node synchronization is ensured.

3.1.1.1 The PWP. The PWP sensor is used to measure the PWP u_w (in Equation 2) at the depth the sensor was buried, in response to the rainfall water infiltration. At the slope with a low groundwater table, the soil is unsaturated. When the rain occurs, the infiltration increases the level of saturation in the soil's depth, and consequently, the hydraulic conductivity increases and the PWP tends to accumulate. In this work, PWP sensors were established at 3, 5, and 11 m, respectively. Accordingly, boreholes were drilled to the slope to install piezometers.

3.1.1.2 The accelerometer sensor. The accelerometer sensor is used to measure both the vibration and the tilt of the slope being considered. For each sensor column, we use three accelerometer sensors to construct a multi-segment inclinometer, in which the distance between two successive sensors is 60 cm. We use pipe segments (the diameter of 0.25 cm and the length of 60 cm) containing an acceleration sensor and an electronics board protected against water by epoxy resin. Signal and power cables inside the pipe are used to connect the electronics board to the main board on the ground. These segments are connected together to form a long column (Uchimura et al. 2015).

3.1.1.3 The soil moisture sensor. The soil moisture sensor is used to measure the volumetric water content of the soil, which is the difference between the air (u_a) and water pressure (u_w) (see u_a and u_w in Equation 2). Depending on the size of the landslide being considered, the number of sensor nodes in the designed network is determined and placed in the slope for measuring and monitoring the slope condition.

3.1.1.4 Microprocessor unit. Microprocessor unit, which is considered as the heart of each sensor node, acquires and packages the data from the sensors. The working stream flow chart is shown in Figure 4(a). The XBee RF module, which is connected directly to the microprocessor unit, receives the data from the microprocessor unit, and then, sends it to the sink node and gateway unit using the star or the tree topologies.

3.1.2 Sink node, gateway unit, and photovoltaic solar panel

These sensor nodes sample and collect the data, and then, package and transfer them to the sink node. The sink node and gateway unit should be located at a safe position near the slope. It is noted that some sensor nodes also act as routers when the network switches from the star to the tree topology. The sink node aggregates the data and sends commands to the sensor nodes. The data are first preprocessed at the sink node and then further forwarded to the Web Server.

The detailed working stream flow of the sink node and the gateway unit is shown in Figure 4(b). The sink node is supplied the power from a battery and a photovoltaic solar panel. When the solar panel's voltage is lower than a defined threshold, a circuit automatically switches power supply to the battery. The gateway transmits the collected data to the Web Server via GSM/GPRS.

3.1.3 The rain gauge and computer station

In this system, a rain gauge is additionally proposed to the system to measure the rain precipitation over a set period of time. The real-time measured data from the rain gauge are transferred to the GeoStudio software at the computer station to model the PWP distribution in the soil slope. Using the SEEP/W module, the flow of water through the unsaturated soil was estimated by using the Darcy's Law (Menció et al. 2014) and Equation 1.

In addition, a WSN software that is developed by the authors is installed at the sink node for the EWM_{RIL} system. This WSN software consists of three modules, data acquisition, data processing, and data communication. The first one is used to record monitoring data from the sensor nodes. The second one is the core component module of the software and is used to process all the incoming monitoring data, and then, sends the command to the sensor nodes. The final module provides the routing algorithms and time synchronization methods (Gutierrez et al. 2001).

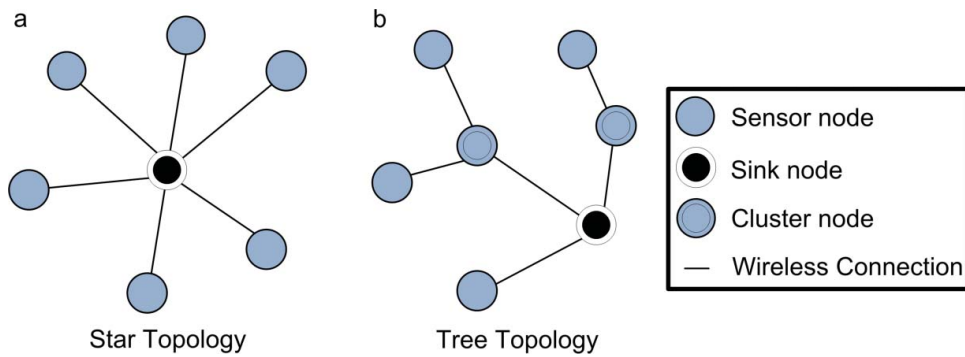


Figure 3. Network topologies used in this study.

3.1.4 Expert and people in change

It is emphasized that the FoS for the slope being considered must be computed beforehand by landslide experts based on the field survey data using the commercial SEEP/W and SLOPE/W software as mentioned in Section 2.1. The near-real-time monitoring data from the sensors mounted in the sensor nodes and the rainfall station are used to compute the near-real-time FoS index (RFoSI). By analyzing FoS and RFoSI, warning messages will be sent to people in charge via the mobile communication network.

3.2. Proposed working principle

3.2.1 Proposed working principle for the wireless sensor nodes and the gateway

Due to the focus of the presented study is on rainfall-induced landslides, the monitoring data are collected and recorded mainly during and after rainfall for saving the energy of the EWM_{RIL} system. In addition, different operating scenarios are also proposed based on rainfall scenarios and corresponding FoSs. More specifically, we defined the two operating scenarios, warning mode and normal mode, based on thresholds computed through an analysis of rainfall and its duration for the slope being considered.

The proposed working principle of the wireless sensor nodes and the sink node in this study is shown in Figure 4. Accordingly, in the normal mode, the sampling rate of the sensors is low. Ts_{old} denotes the sampling value being set at the sensor nodes, whereas Ts_{new} denotes new sampling values that workstation required sensor nodes change to. The value of Ts_{new} and Ts_{old} are preset values Ts_1 , Ts_2 , or Ts_3 (see Figure 5). It is noted that $Ts_1 > Ts_2 > Ts_3$, which means that the sampling frequency increases as the FoS value decreases. A change in sampling rate depends on the result of slope stability analysis. The value of the sampling rate is varied depending on the FoS to meet two purposes: reducing the number of samples to be transmitted in the case of the slope is safe or increasing the collected data when the slope is unsafe. Thus, the warning mode will be activated if Ts_{new} is less than Ts_1 , and for this case, the network topology is switched from the tree topology to the star topology. Accordingly, the sampling rate of the monitoring data is increased from $1/Ts_{old}$ to $1/Ts_{new}$ samples per second. If Ts_{new} equals Ts_1 , the network topology is switched from the star topology to the tree topology to save the energy (Nguyen et al. 2015).

3.2.2 Proposed working principle for the instability prediction and the real-time warning

The proposed working principle of the instability prediction and the real-time warning is shown in Figure 5. Threshold₀ is an empirical pre-set value of rainfall intensity. In our work, Threshold₀ is determined based on the formula proposed by Guzzetti et al. (2008). If the rainfall reaches this threshold, the system will send a notification to the operating expert suggesting that a slope stability analysis should be performed. If the rainfall intensity is lower than Threshold₀, the operation of

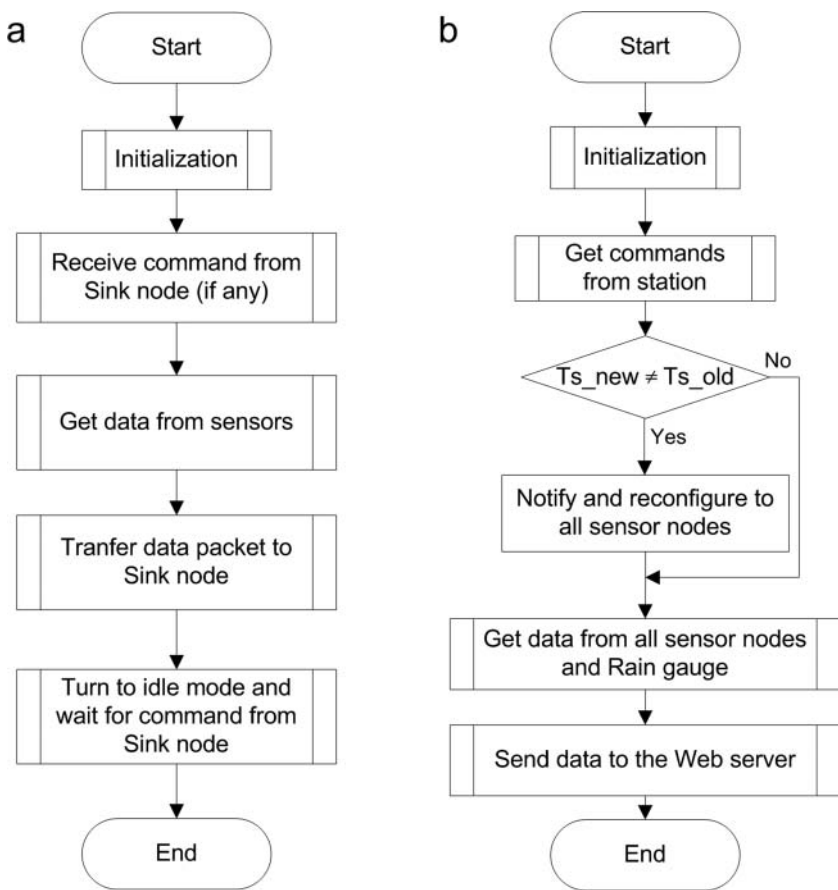


Figure 4. The proposed working principle in this research: (a) the wireless sensor nodes and (b) the sink node and gateway unit.

the system depends on its current operating status, in the warning state or not. For example, although the rainfall intensity is lower than the threshold₀, the slope is in an unstable state because of high PWP, the system will send a notification to the operating expert. If the slope is in stability status and the rainfall intensity is below Threshold₀, there is no need to evaluate the landslide hazard. It should be noted that the warning state is a binary variable, ‘1’—warning state, whereas ‘0’—safe state. The value of this variable defaults to 0 and would be set to 1 (if $FoS \leq Threshold_1$) or 0 (if $FoS > Threshold_1$) after analyzing the slope stability.

In our proposed scheme, besides the geotechnical properties and the topography of the slope, the input data for the FoS analysis are (i) the rainfall and rain intensity from the gauge station; and (ii) the monitoring data from the field site. Thus, PWP is not only the input data but also the parameter for evaluating the result of the model simulation. Accordingly, the operating expert uses the weather forecast data to evaluate the stability of the slope in the near future. It is noted that the greater the FoS is, the steadier the slope is. A warning for the landslide is announced if the simulation result of FoS is low. We define Threshold₁ and Threshold₂ for FoS of the slope based on analysis of the slope combined with empirical knowledge of our geotechnics experts. These thresholds are corresponding to the two warning levels (early, intermediate), however, these thresholds should be updated by experts during the operation. If FoS is lower than Threshold₁ or Threshold₂, the slope is in an instability state, and therefore, the warning (early or intermediate) is issued. The time period from this instability state to the landslide occurrence (FoS reaching to 1) is coded as Nd. For this purpose, a simulation test has been carried out using the slope’s data and the forecast rainfall to



determine Nd. Based on Nd, the operating expert could make a suitable decision. Thus, if the slope is predicted as unstable, the sensors will switch to the higher sampling rate, and vice versa, if FoS is higher than Threshold_1, the system will switch to the normal state, in which the sample rate used is lower to reduce the power consumption of the sensor nodes.

If $FoS < \text{Threshold_1}$ (the slope is in a warning state, low stability or vibrations), the system will switch to the tree topology mode. In this mode, the high sample rate and the high transfer rate are

activated to sense the data of the slope. The sensor nodes will reconfigure themselves to communicate directly with the sink node. Using the sensed data, the FoS will be estimated. In case the slope turns back to the safe state (FoS increase), the system will switch from the star topology to the tree topology, and in this case, the sensor nodes will turn into the idle mode to save energy. The power for the sensors will be turned off, and the Wasmote board and the RF module also switch to the idle mode.

For the case of the landslide happen, a pre-determined vibration threshold (Threshold_3) must be properly selected. According to Kotta et al. (2011), the vibration value on the X and Y axes of an acceleration sensor in a position on the ground above 0.5 g indicates a remarkable ground movement. Uchimura et al. (2015) suggested that if a slope has a tilting rate of 0.010 per hour, a precaution should be issued. Therefore, in this project, we designed the Threshold_3 = 0.5 g ($1\text{ g} = 9.8\text{ m/s}^2$). Accordingly, if the vibrations in at least two nodes reach the Threshold_3 mean that the landslide is happening and a warning message at the imminent level is sent to the person in charge.

4. The case study for the proposed EWM_{RIL}

4.1 Data collection and processing

In this research, the Nam Dan landslide in Xin Man district, Ha Giang province, located in the northern mountainous region of Vietnam was selected as a case study. Xin Man is a highland district in the western part of Ha Giang province, characterized by strong dissection of topography, steep slopes, many high mountains, and prone to landslides. The elevation varies from 500 to 1700 m. Valleys are very steep, deep, and characteristic V-sharps. Large sliding blocks appear along the roads where sloping roofs are severely cut and at the foot of mountains there is a runoff. This district covers an area of 582 km² and is currently considered to be one of the most prone landslide areas in Vietnam. Statistics of the historical landslides recorded in Xin Man shows a total of 967 landslides occurred from 2012 to 2016 (Ngoc et al. 2016).

The average rainfall is around 1695 mm yearly. Rainfall is particularly high during August and September. This is considered the main triggering factor that causes flash floods, debris flows, and landslides in the area.

Nam Dan landslide is located along the road 178. The reactive landslide under investigation has the highest altitude reaching 870 m above sea level and faces West to East. The Nam Dan landslide is approximately 360 m long from the detected open crack to its toe (Figure 6). The depth and the average width of the landslide are around 30 and 245 m, respectively. The slope is from 26° to 45° degrees. The slope surface is covered with a layer of clay mixed with yellowish residual weathering macadam. Underneath is the bedrock belonging to the Song Chay complex – Phase 2 ($\gamma\text{aD}_1\text{sc}_2$) where the main lithology is coarse grained gneissoid biotite granites. On the top of this bedrock layer, the bedrock has been weathering in moderately to strongly, whereas, at the bottom, the bedrock acts as a water blocking layer. The topsoil and weathered rock are affected by infiltration. A typical cross-section of the landslide is shown in Figure 7(a) and two photos of the landslide taken on 15 May 2016 are shown in Figure 7(b,c).

In this research, four laboratory tests, the physical properties test, the pressure plate test, the direct shear test, and the triaxial test were conducted to acquire physical and mechanical parameters for each layer. In addition, the parameter of residual strength of soil was determined using Bishop-type ring shear test (Bishop et al. 1971). Furthermore, a series of field investigations were carried out from May–August 2016 where detailed information of the landslide i.e. heights, angle, lower length, upper length, and slip surface characteristics were determined, and the soil samples were collected at the slope. These samples were then analyzed at the geotechnical laboratory to determine geotechnical properties such as soil classification, water content, soil–water characteristic curves, and shear strength.

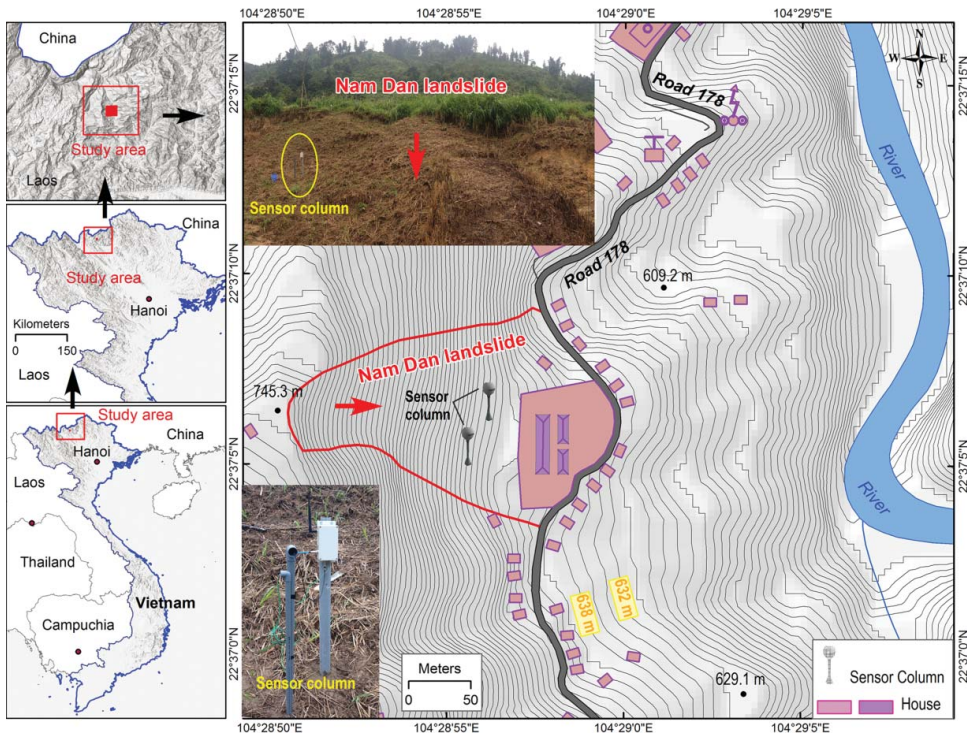


Figure 6. Location the Nam Dan landslide; (a) a photo of the sensor column position; (b) a photo of the sensor column used in this project.

It is noted that the Unified Soil Classification System (ASTM Committee D-18 on Soil and Rock 2011) was adopted to classify the soils, whereas Landes and Begley (1976) was used for the soil samples testing. Using the four laboratory tests mentioned above, the geotechnical properties of the slope were determined: the cohesion is 23 (kPa), unit weight is 16.5 (kN/m³), volumetric water content is 0.36 (m³/m³), hydraulic conductivity is 0.65 (m/day), and residual water content is 0.2 (m³/m³) (Figure 7(a)). These geotechnical properties of the slope were then used to calculate FoS using the SEEP/W and SLOPE/W modules in the GeoStudio software.

4.2 The EWM_{RIL} for the Nam Dan landslide

For early warning and monitoring system of the landslide, we designed a total of six WSN nodes for the monitoring network. Each sensor node consists of a Wasp mote board, a battery, a XBee module, a soil moisture sensor, three PWP sensors, and three 3-DOF (degree of freedom) acceleration sensors as shown in Figure 2. The data acquired from sensor nodes and rain gauge are sent to the sink node and then transmitted wirelessly through GSM/GPRS module to a MySQL database on a Web Server. A web application and an Android application are also built for remote monitoring (Figure 8(a,b)). The users can monitor the vibration, the tilt, and the displacement estimated using acceleration data (Figure 8(c)).

It is noted that this is a season effect Nam Dan landslide where the initial conditions used for the FEM, i.e. pore-water pressures and hydraulic conductivity of soil are dependent on the rainfall season, from May to October yearly.

Figure 9 shows the seepage estimation at different times with the uniform rainfall intensity of 200 mm/day for 15 days. Due to the infiltration of rainwater, the groundwater level increases gradually from the first day to the 15th day. It can be seen that the pore pressure level rises day by day.

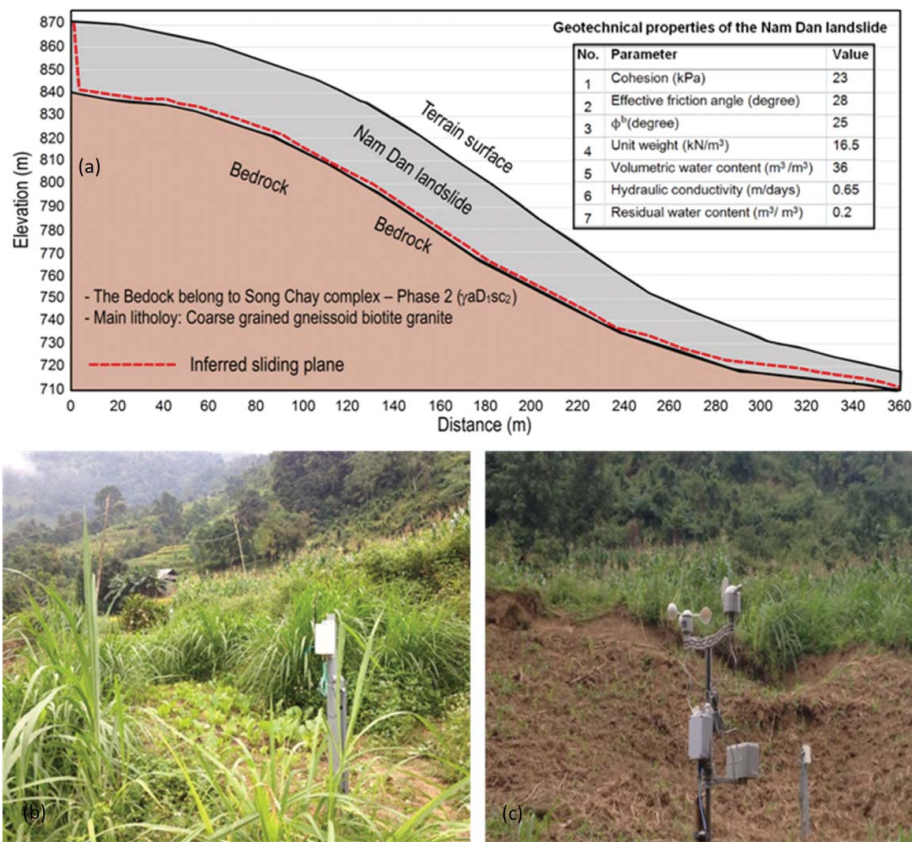


Figure 7. (a) Cross section and (b) and (c) two photos (taken by Tran Duc-Tan on 15 May 2016) of the Nam Dan landslide.

In Figure 10, with the average rainfall intensity of 200 mm/day, the FoS dropped to 0.877 (i.e. warning level) after 15 days. When rainfall infiltrated the soil layer, the matric suction gradually decreased, the groundwater level gradually increased resulting in reduced shear strength. The FoS decreased with time of rainfall. On the 15th day, the FoS reached 0.877. The critical slip surface changes over time depending on the distribution of matric suction. It is noted that the agreement between the measured values of PWP at the field site and the estimated values of PWP from the simulation confirms the reliability of our evaluation about the slope stability.

Figure 11 shows more details about the dependence of FoS on rainfall intensity over time. Figure 11(a) presents two cases of rainfall: uniform and non-uniform intensities with a note that the total rainfall is the same. We assume that the uniform intensity of the rainfall (i.e. dotted curve) is the initial input of the FEM simulation. If we can exploit the rainfall intensity from the rain gauge as shown in the solid curve, the estimation of the FoS would be different. In detail, at the 12th day, the scenario with a uniform intensity of the rainfall still showed that the slope was safe (i.e. $FoS > 1$). The FoS dropped to below 1 (i.e. warning level) after 12 days. However, the scenario with the non-uniform rainfall intensity showed that the slope is not safe anymore on the 12th day (i.e. $FoS < 1$). In both cases, it can be seen that the slope stability decreased as the rain duration increased. The value of FoS significantly reduced in a linear trend when the rain duration increased from the first day until the 12th day. However, the FoS declines slowly after the 13th day. As described in the above section, the groundwater at the landslide site is mainly located in the fractured weathered bedrock. Most rainfall may flow downwards to the hillside through the fractures and difficult to remain in the pore space.

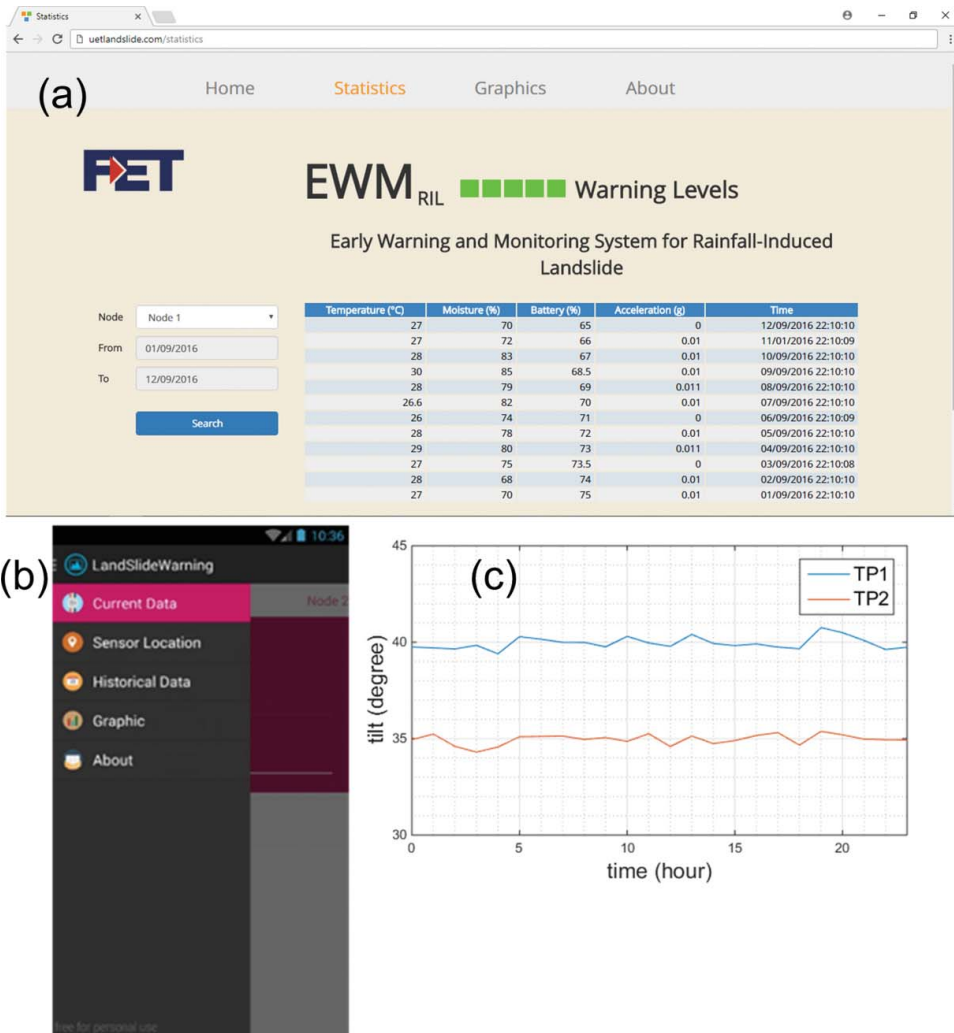


Figure 8. Data monitoring through our website (a); our mobile application (b) and an example of tilt estimated using acceleration data (c).

5. Concluding remark

This paper proposed and implemented an EWM_{RIL} with a case study at the Nam Dan landslide, Xin Man district, northern Vietnam, in which, a detailed explanation of the technical design of the EWM_{RIL} system is provided. According to current literature, such kind of an explanation has seldom been provided. Therefore, the work could partially fill this shortage in literature.

The proposed EWM_{RIL} is an integrated system that combines a wireless sensor network, the FES analysis, and the limit equilibrium slope stability analysis for a real-time early warning and monitoring of the landslide. Accordingly, the instability status of the slope was determined based on FoS that was calculated using its parameters derived in the fieldwork. These parameters are monitored real time and sent to the computer station to compute FoS. Based on the computed FoS, the status of the slope was analyzed, and then, decision-making could be issued.

The advantage of the proposed system is that flexible and reliable WSN are introduced to adapt to the designed warning state of the landslide. Consequently, the system is more balanced between the power saving and the reliability. In Nguyen and Tran et al. (2015), the network is switched from

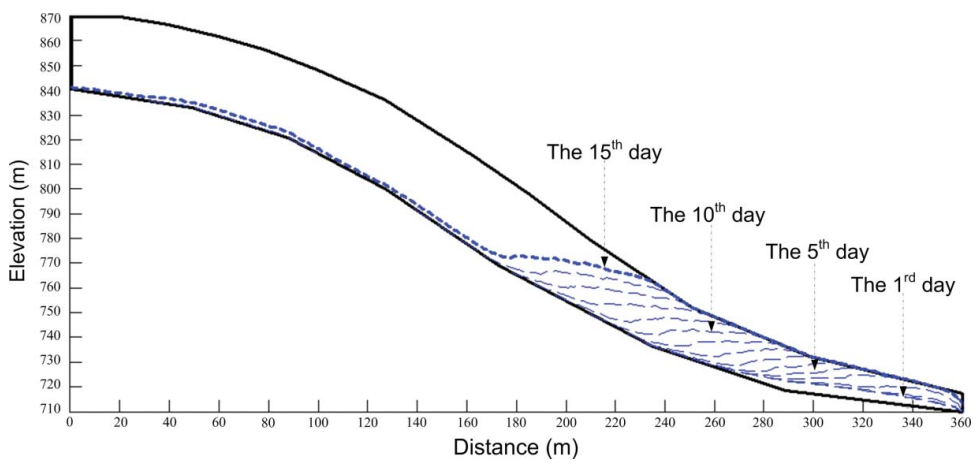


Figure 9. Seepage estimation for the Nam Dan landslide at different times.

the tree topology to the star topology when the rainfall reaches to the determined threshold, even though the FoS is still high (i.e. $FoS \gg 1$). In our work, the WSN system only switches from the tree topology to the star topology when FoS reaches to a warning threshold. Thus, the proposed system in this research is more effective than that in the previous works, i.e. in (Nguyen and Tran et al. 2015) in terms of the power consumption.

One of the critical problems in an EWM_{RIL} landslide is that some sensor nodes buried in the slope may be broken or destroyed or out of work due to the moving of the landslide or other errors, therefore, reducing the reliability of the system. In this study, the proposed system is capable to automatically switch from the tree topology to the star topology when the slope is in unstable status. Therefore, if some sensor nodes are broken, the other sensor nodes will continue working, and thus, the reliability of the system could be preserved.

Besides the proposed flexible configuration of the system, a new working principle for the wireless sensor nodes and the gateway has also been proposed. Accordingly, two operating

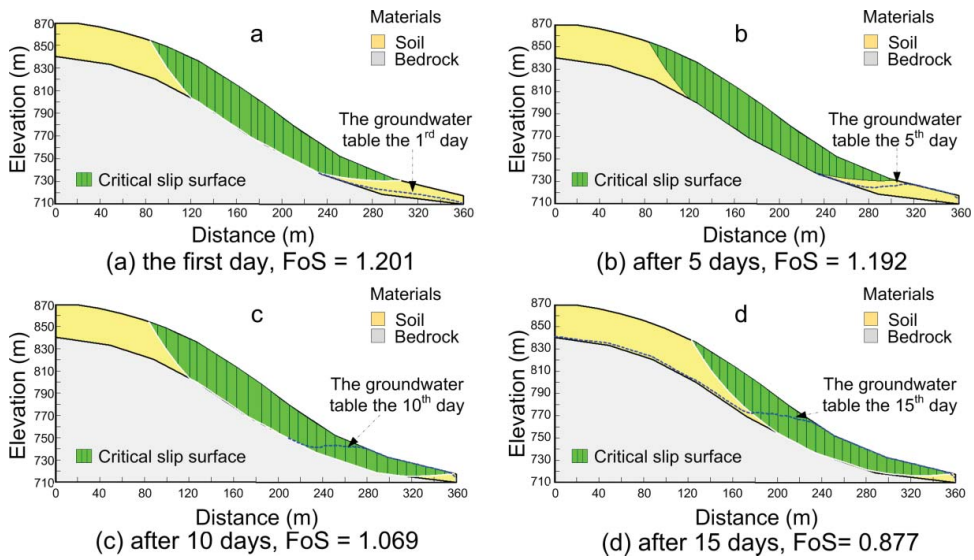


Figure 10. The changing of FoS correlates with the seepage estimation at the same time of the slope for 15 days with the rain intensity of 200 mm/day.

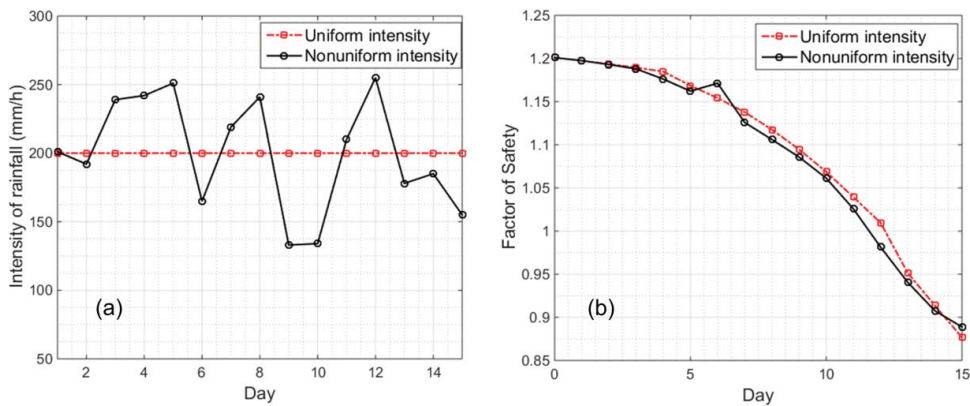


Figure 11. (a) Intensity of rainfall vs. time; (b) Critical slip surface FoS vs. time.

scenarios, the warning mode with the designed high sampling rate and the normal mode with the designed low sampling rate, therefore, the power consumption is lower than that at the regular working principle.

The main limitation of the proposed system in this work is that the EWM_{RIL} system is feasible for site-scale rainfall-induced landslides. In addition, the system requires a detailed geotechnical investigation to establish FoS, therefore, this may be a cost-consuming system, especially for large landslides. Furthermore, due to the natural limitation of the current sensor and wireless technology in terms of power consumption, more power-efficient solutions should be further considered in the future to improve the EWM_{RIL} system.

It is noted that we proposed to use the ZigBee and flexible topologies based on the size of the Nam Dan landslide, where the communication range is around 300 m. Therefore, for larger communication ranges, other wireless communication technologies such as LoRaWan (Augustin et al. 2016) could be considered.

At the final conclusion, despite some aforementioned limitations, the result of this research is useful for landslide risk prevention and management in landslide prone-areas.


Acknowledgments


The analysis and write-up were carried out as a part of the first author's PhD studies at Faculty of Electronics and Telecommunication, VNU University of Engineering and Technology, Hanoi, Vietnam. We would like to thank two anonymous reviewers for their valuable comments.


Disclosure statement

The authors declare no conflict of interest.

ORCID

Quoc Anh Gian  <http://orcid.org/0000-0003-1439-3469>

Duc-Tan Tran  <http://orcid.org/0000-0002-7673-388X>

Dieu Tien Bui  <http://orcid.org/0000-0001-5161-6479>

References

- Ahlheim M, Frör O, Heinke A, Keil A, Nguyen MD, Pham VD, Saint-Macary C, Zeller M. 2008. Landslides in mountainous regions of Northern Vietnam: causes, protection strategies and the assessment of economic losses. Report No. Nr.298/2008. Stuttgart, Germany: University of Hohenheim.

- Angeli M-G, Pasuto A, Silvano S. 2000. A critical review of landslide monitoring experiences. *Eng Geol.* 55(3):133–147.
- ASTM Committee D-18 on Soil and Rock. 2011. Standard practice for classification of soils for engineering purposes (unified soil classification system). Philadelphia, PA: ASTM International.
- Augustin A, Yi J, Clausen T, Townsley WM. 2016. A study of LoRa: long range & low power networks for the internet of things. *Sensors* 16(9):1466.
- Ávila A, Justino F, Wilson A, Bromwich D, Amorim M. 2016. Recent precipitation trends, flash floods and landslides in southern Brazil. *Environ Res Lett.* 11(11):114029.
- Barla M, Antolini F. 2016. An integrated methodology for landslides' early warning systems. *Landslides* 13(2):215–228.
- Baronti P, Pillai P, Chook VW, Chessa S, Gotta A, Hu YF. 2007. Wireless sensor networks: a survey on the state of the art and the 802.15. 4 and ZigBee standards. *Comput Commun.* 30(7):1655–1695.
- Baum RL, Godt JW. 2010. Early warning of rainfall-induced shallow landslides and debris flows in the USA. *Landslides* 7(3):259–272.
- Bhattacharya S, Krishna AM, Lombardi D, Crewe A, Alexander N. 2012. Economic MEMS based 3-axis water proof accelerometer for dynamic geo-engineering applications. *Soil Dyn Earthq Eng.* 36:111–118.
- Bishop AW, Green G, Garga VK, Andresen A, Brown J. 1971. A new ring shear apparatus and its application to the measurement of residual strength. *Geotechnique* 21(4):273–328.
- Calvello M, Picciullo L. 2016. Assessing the performance of regional landslide early warning models: the EDuMaP method. *Nat Hazard Earth Syst Sci.* 16(1):103–122.
- Capparelli G, Versace P. 2011. FLAIR and SUSHI: two mathematical models for early warning of landslides induced by rainfall. *Landslides* 8(1):67–79.
- Chae B-G, Kim M-I. 2012. Suggestion of a method for landslide early warning using the change in the volumetric water content gradient due to rainfall infiltration. *Environ Earth Sci.* 66(7):1973–1986.
- Collins BD, Znidarcic D. 2004. Stability analyses of rainfall induced landslides. *J Geotech Geoenviron Eng.* 130(4):362–372.
- Cuomo F, Della Luna S, Todorova P, Suihko T. 2008. Topology formation in IEEE 802.15. 4: cluster-tree characterization. In: Mutka M, editor. *Proceedings of the Sixth Annual IEEE International Conference on Pervasive Computing and Communications, PerCom 2008*; March 17–21; Hong Kong, China. Los Alamitos (CA): IEEE Computer Society. p. 276–281.
- Del Soldato M, Bianchini S, Calcaterra D, De Vita P, Martire DD, Tomás R, Casagli N. 2017. A new approach for landslide-induced damage assessment. *Geomatics, Nat Hazards Risk.* 1–14. Available from: http://www.tandfonline.com/doi/full/10.1080/19475705.2017.1347896?utm_source=TrendMD&utm_medium=cpc&utm_campaign=Geomatics%252C_Natural_Hazards_and_Risk_TrendMD_1
- Deng T, Chen D, Wang J, Chen J, He W. 2014. A MEMS based electrochemical vibration sensor for seismic motion monitoring. *J Microelectromech Syst.* 23(1):92–99.
- Dou J, Tien Bui D, P. Yunus A, Jia K, Song X, Revhaug I, Xia H, Zhu Z. 2015. Optimization of causative factors for landslide susceptibility evaluation using remote sensing and GIS data in parts of Niigata, Japan. *PLoS One.* 10(7): e0133262.
- Elson J, Girod L, Estrin D. 2002. Fine-grained network time synchronization using reference broadcasts. *ACM SIGOPS Operating Syst Rev.* 36(SI):147–163.
- Fosalau C, Zet C, Petrisor D. 2016. Implementation of a landslide monitoring system as a wireless sensor network. *Proceedings of the 7th Annual Ubiquitous Computing, Electronics & Mobile Communication Conference (UEMCON 2016)*; October 20–22, New York, NY: IEEE. p. 1–6.
- Fredlund D, Morgenstern NR, Widger R. 1978. The shear strength of unsaturated soils. *Can Geotech J.* 15(3):313–321.
- Greco R, Guida A, Damiano E, Olivares L. 2010. Soil water content and suction monitoring in model slopes for shallow flowslides early warning applications. *Phys Chem Earth* 35(3–5):127–136.
- Gutierrez JA, Naeve M, Callaway E, Bourgeois M, Mitter V, Heile B. 2001. IEEE 802.15. 4: a developing standard for low-power low-cost wireless personal area networks. *IEEE Netw.* 15(5):12–19.
- Guzzetti F, Peruccacci S, Rossi M, Stark CP. 2008. The rainfall intensity–duration control of shallow landslides and debris flows: an update. *Landslides* 5(1):3–17.
- Hons M, Stewart R, Lawton D, Bertram M, Hauer G. 2008. Field data comparisons of MEMS accelerometers and analog geophones. *Leading Edge.* 27(7):896–903.
- Intrieri E, Gigli G, Mugnai F, Fanti R, Casagli N. 2012. Design and implementation of a landslide early warning system. *Eng Geol.* 147:124–136.
- Kirschbaum D, Adler R, Hong Y, Lerner-Lam A. 2009. Evaluation of a preliminary satellite-based landslide hazard algorithm using global landslide inventories. *Nat Hazard Earth Syst Sci.* 9(3):673–686.
- Kjekstad O, Highland L. 2009. Economic and social impacts of landslides. In: Sassa K, Canuti P, editors. *Landslides – disaster risk reduction*. Berlin: Springer; p. 573–587.

- Klose M, Damm B, Terhorst B. 2015. Landslide cost modeling for transportation infrastructures: a methodological approach. *Landslides* 12(2):321–334.
- Kotta HZ, Rantelobo K, Tena S, Klau G. 2011. Wireless sensor network for landslide monitoring in Nusa Tenggara Timur. *TELKOMNIKA (Telecommun Comput Electron Control)* 9(1):9–18.
- Krahn J. 2012a. Seepage modeling with SEEP/W: an engineering methodology. Calgary: GEO-SLOPE International Ltd.
- Krahn J. 2012b. Stability modeling with SLOPE/W: an engineering methodology. Calgary: GEO-SLOPE International Ltd.
- Lagomarsino D, Segoni S, Fanti R, Catani F. 2013. Updating and tuning a regional-scale landslide early warning system. *Landslides* 10(1):91–97.
- Landes JD, Begley JA. 1976. Mechanics of crack growth, ASTM STP 590. Philadelphia: American Society for Testing and Materials, p. 128–148.
- Liao ZH, Hong Y, Wang J, Fukuoka H, Sassa K, Karnawati D, Fathani F. 2010. Prototyping an experimental early warning system for rainfall-induced landslides in Indonesia using satellite remote sensing and geospatial datasets. *Landslides* 7(3):317–324.
- Lin M-L, Lin S-C, Lin Y-C. 2016. Review of landslide occurrence and climate change in Taiwan, slope safety preparedness for impact of climate change. In: Ken H, Lacasse S, Picarelli L, editors. *Slope safety preparedness for impact of climate change*. Leiden: CRC Press, p. 409–436.
- Liu S, Shao L, Li H. 2015. Slope stability analysis using the limit equilibrium method and two finite element methods. *Comput Geotech*. 63:291–298.
- Loi DH, Quang LH, Sassa K, Takara K, Dang K, Thanh NK, Van Tien P. 2017. The 28 July 2015 rapid landslide at Ha Long City, Quang Ninh, Vietnam. *Landslides* 14(3):1207–1215.
- López G, Moura P, Moreno J, Camacho J. 2014. Multi-faceted assessment of a wireless communications infrastructure for the green neighborhoods of the smart grid. *Energies* 7(5):3453–1215.
- Macciotta R, Hendry M, Martin CD. 2016. Developing an early warning system for a very slow landslide based on displacement monitoring. *Nat Hazards*. 81(2):887–907.
- Manconi A, Giordan D. 2015. Landslide early warning based on failure forecast models: the example of the Mt. de La Saxe rockslide, northern Italy. *Nat Hazards Earth Syst Sci*. 15(7):1639–1644.
- Manual Product. 2008. Xbee Znet 2.5/Xbee PRO Znet 2.5 OEM RF Modules. Digi International Inc.
- Mathew J, Babu DG, Kundu S, Kumar KV, Pant CC. 2014. Integrating intensity-duration-based rainfall threshold and antecedent rainfall-based probability estimate towards generating early warning for rainfall-induced landslides in parts of the Garhwal Himalaya, India. *Landslides* 11(4):575–588.
- Menció A, Galán M, Boix D, Mas-Pla J. 2014. Analysis of stream–aquifer relationships: a comparison between mass balance and Darcy’s law approaches. *J Hydro*. 517:157–172.
- Ngoc DM, Thuy DT, Duc DM. 2016. [Application of GIS and analytic hierarchy process for mapping landslide risks at Xin Man district, Ha Giang province, Vietnam]. *VNU J Sci: Earth Environ Sci*. 32(2S):206–216. Vietnamese.
- Nguyen CD, Tran TD, Tran ND, Huynh TH, Nguyen DT. 2015. Flexible and efficient wireless sensor networks for detecting rainfall-induced landslides. *Int J Distrib Sens Netw*. 11(11):1–13.
- Nguyen D-C, Duc-Tan T, Tran D-N. 2015. Application of compressed sensing in effective power consumption of WSN for landslide scenario. *Proceedings of the 2015 Asia Pacific Conference on Multimedia and Broadcasting (APMediaCast)*; April 23–25; Bali, Indonesia. IEEE Communications Society, p. 1–5.
- Papa MN, Medina V, Ciervo F, Bateman A. 2013. Derivation of critical rainfall thresholds for shallow landslides as a tool for debris flow early warning systems. *Hydrol Earth Syst Sci*. 17(10):4095–4107.
- Pham BT, Bui DT, Pham HV, Le HQ, Prakash I, Dholakia M. 2017. Landslide hazard assessment using random subspace fuzzy rules based classifier ensemble and probability analysis of rainfall data: a case study at Mu Cang Chai District, Yen Bai Province (Vietnam). *J Indian Soc Remote Sens*. 45(4):673–683.
- Quecedo M, Pastor M, Herreros M, Fernández Merodo J. 2004. Numerical modelling of the propagation of fast landslides using the finite element method. *Int J Numer Meth Eng*. 59(6):755–794.
- Rahardjo H, Nio AS, Leong EC, Song NY. 2010. Effects of groundwater table position and soil properties on stability of slope during rainfall. *J Geotech Geoenviron Eng*. 136(11):1555–1564.
- Rahimi A, Rahardjo H, Leong E-C. 2010. Effect of hydraulic properties of soil on rainfall-induced slope failure. *Eng Geol*. 114(3):135–143.
- Ramesh MV. 2014. Design, development, and deployment of a wireless sensor network for detection of landslides. *Ad Hoc Netw*. 13:2–18.
- Rawat P, Singh KD, Chaouchi H, Bonnin JM. 2014. Wireless sensor networks: a survey on recent developments and potential synergies. *J Supercomput*. 68(1):1–48.
- Saito H, Korup O, Uchida T, Hayashi S, Oguchi T. 2014. Rainfall conditions, typhoon frequency, and contemporary landslide erosion in Japan. *Geology* 42(11):999–1002.
- Schuster RL, Fleming RW. 1986. Economic losses and fatalities due to landslides. *Bull Assoc Eng Geol*. 23(1):11–28.

- Terlien MT. 1998. The determination of statistical and deterministic hydrological landslide-triggering thresholds. *Environ Geol.* 35(2):124–130.
- Thiebes B, Bell R, Glade T, Jager S, Mayer J, Anderson M, Holcombe L. 2014. Integration of a limit-equilibrium model into a landslide early warning system. *Landslides* 11(5):859–875.
- Tien Bui D, Anh Tuan T, Hoang N-D, Quoc Thanh N, Nguyen BD, Van Liem N, Pradhan B. 2017. Spatial prediction of rainfall-induced landslides for the Lao Cai area (Vietnam) using a novel hybrid intelligent approach of least squares support vector machines inference model and Artificial Bee Colony optimization. *Landslides* 14(2):447–458.
- Tien Bui D, Nguyen Q-P, Hoang N-D, Klempe H. 2017. A novel fuzzy K-nearest neighbor inference model with differential evolution for spatial prediction of rainfall-induced shallow landslides in a tropical hilly area using GIS. *Landslides* 14:1–17.
- Tien Bui D, Pradhan B, Lofman O, Revhaug I, Dick O. 2013. Regional prediction of landslide hazard using probability analysis of intense rainfall in the Hoa Binh province. *Vietnam Nat Hazards* 66(2):707–730.
- Tien Bui D, Pradhan B, Nampak H, Quang Bui T, Tran Q-A, Nguyen QP. 2016. Hybrid artificial intelligence approach based on neural fuzzy inference model and metaheuristic optimization for flood susceptibility modelling in a high-frequency tropical cyclone area using GIS. *J Hydrol.* 540:317–330.
- Trezzini F, Giannella G, Guida T. 2013. Landslide and flood: economic and social impacts in Italy. In: Margottini C, Canuti PSK, editors. *Landslide science and practice*. Berlin: Springer; p. 171–176.
- Uchimura T, Towhata I, Wang L, Nishie S, Yamaguchi H, Seko I, Qiao J. 2015. Precaution and early warning of surface failure of slopes using tilt sensors. *Soils Found.* 55(5):1086–1099.
- UN-ISDR. 2006. Developing early warning systems: a checklist. Third International Conference on Early Warning (EWC III). United Nation/ International Strategy for Disaster Reduction (UN/ISDR), 27–29 March 2006, Bonn, Germany.
- Wood J, Harrison S, Turkington T, Reinhardt L. 2016. Landslides and synoptic weather trends in the European Alps. *Climatic Change* 136(2):297–308.
- Xie Q-M, Bian X, Xia Y-Y. 2005. Systematic analysis of risk evaluation of landslide hazard. *Yantu Lixue(Rock Soil Mech)*. 26(1):71–74.
- Yin Y, Wang H, Gao Y, Li X. 2010. Real-time monitoring and early warning of landslides at relocated Wushan Town, the Three Gorges Reservoir, China. *Landslides* 7(3):339–349.